Hindawi
Nanomaterials and Nanotechnology
Volume 2023, Article ID 9753824, 11 pages
https://doi.org/10.1155/2023/9753824

Research Article

Characterization of Bismuth Composited to Carbon Nanotube-Coated Titanium Cathode in Electro-Fenton System

Yi-Ta Wang,[1] **Yi-Chi Hsieh**,[1] **and Yue-Sheng Lin**[2]

[1]*Department of Mechanical and Electromechanical Engineering, National I-Lan University, Yilan County, Yilan 26047, Taiwan*
[2]*Department of Mechanical Engineering, National Taiwan University of Science and Technology, Taipei City 10607, Taiwan*

Correspondence should be addressed to Yi-Ta Wang; ytwang@niu.edu.tw

Received 15 June 2022; Accepted 16 January 2023; Published 14 August 2023

Academic Editor: Leander Tapfer

Bismuth (Bi) is a highly reactive catalyst for the generation of hydroxyl (•OH) radicals. Cathodes constructed from composites of Bi and carbon nanotube (CNT) exhibit high stability and low resistance, which enhance their electron transfer capability. In this work, a titanium substrate was coated with multi-walled carbon nanotube (MWCNT/Ti) using electrophoretic deposition process, followed by electrodeposition of Bi onto the MWCNT-coated Ti (Bi/MWCNT/Ti). The effects of Bi electrodeposition time on the surface morphology of Bi/MWCNT/Ti cathodes were investigated by scanning electron microscopy and energy-dispersive X-ray spectroscopy, and the electrochemical characteristics of each cathode were identified via a series of electrochemical analyses further. The results demonstrated that electrodeposition at −0.85 V vs. Ag/AgCl for 5 min revealed uniform distribution of dense Bi across the surface of cathode, which provides better hydrophilicity for cathode and promotes highest electron transfer rates, respectively; when the Bi/MWCNT/Ti cathode was used as an electro-Fenton (EF) cathode, the EF system achieved a rhodamine B degradation rate of 80.8% after 30 min, which is a significant increase (83.63%) than the unmodified Ti cathode. The use of Bi in EF cathodes improves the efficiency of the EF process.

1. Introduction

In advanced oxidation processes (AOPs), external voltage is applied to generate reactive species like hydroxyl radicals (·OH), which degrade or mineralize organic materials. Thus, AOPs can be conducted to remove pollutants from wastewater. Moreover, they are cost-effective as they do not require special equipment [1]. The electro-Fenton (EF) process has been studied extensively since its discovery in 1987; in essence, it is a combination of Fenton chemistry and electrochemistry. The EF process is based on Fenton's reagent, which is a mixture of hydrogen peroxide (H_2O_2) and ferrous iron (Fe^{2+}). Through the application of external potential, H_2O_2 is generated from the cathode, while Fe^{3+} is reduced to Fe^{2+} at the anode. This results in the production of highly reactive •OH species that oxidatively degrade organic pollutants [2]. The reactions of the EF process are shown in equations (1)–(3).

$$O_2 + H^+ + 2e^- \longrightarrow H_2O_2 \quad (1)$$

$$Fe^{2+} + H_2O_2 \longrightarrow Fe^{3+} + OH^- + \bullet OH \quad (2)$$

$$Fe^{3+} + e^- \longrightarrow Fe^{2+} \quad (3)$$

The cathode is an important component of the EF system and governs the efficiency of the system. They must also exhibit high oxygen reducing reaction (ORR) activity and possess a high hydrogen evolution reaction (HER) overpotential to prevent undesirable side reactions [3, 4]. Sirés and Brillas [5] showed that carbonaceous materials (e.g., commercial graphite felt, carbon felt, and carbon sponges) are the most common types of electrodes for EF systems. However, they are less conductive than metals and not suitable to additional processing owing to their mechanically unstable nature [6]. Metals are highly conductive and amenable to processing because of which they can withstand

modifications to improve cathode performance and extend the service life. Titanium (Ti) is electrochemically stable and intrinsically resistant to corrosion when used in cathodes [6]. Furthermore, Ti is a low-performance HER catalyst [7], which helps prevent side reactions. Sun et al. [8] used Ti/PbO_2 composite electrodes to electrochemically treat malachite green-containing wastewaters and achieved 97.70% removal after 240 min. Yuan et al. [9] experimentally studied the effects of current on H_2O_2 generation in Ti/MMO working electrodes; they revealed that Ti/MMO electrodes exhibit high surface currents, which facilitate electron exchange between O_2 species and the cathode to promote H_2O_2 generation. In summary, Ti shows excellent promise as a material for working electrodes in AOPs, and Ti electrodes whose surfaces have been modified to incorporate catalytic materials can be used in EF systems.

Carbon nanotube (CNT) is known for possessing several unique characteristics and has been used in various applications related to materials science. For example, CNT is widely employed in fuel cells, as CNT-modified electrodes typically outperform unmodified electrodes. In studies about fuel cell electrodes, it has been demonstrated that fuel cell performance can be improved through the use of CNT composites as electrodes or catalysts owing to their unique pore structure; nanometer-scale dimensions; high conductivity, chemical stability, and mechanical strength; large specific surface area; and ductility [10]. Therefore, CNTs have significant potential as electrode materials in other systems. For instance, Roth et al. developed a tubular CNT-based gas diffusion electrode, which achieved a decolorization rate of 96% with wastewaters containing the Acid Red 14 dye [11]. Khataee et al. compared the reactivity of bare and CNT-coated graphite electrodes toward the generation of H_2O_2 and found that the CNT-modified electrode outperformed the unmodified electrode. This result was attributed to the high catalytic activity and large specific surface area of CNT [12]. Therefore, CNT electrodes exhibit high performance when used in a variety of applications.

Bismuth (Bi) has high carrier mobility [13] and high HER overpotential [14]; it has been shown that modification with Bi improves hydrophilicity [15] and electrochemical oxidation activity [16]. Bi can also react with H_2O_2 to form highly reactive •OH radicals. Jeromiyas et al. [17] fabricateda three-dimensional hierarchical network comprising Bi nanoparticles and graphene-carbon nanotubes (Bi NPs@Gr-CNTs). They demonstrated that the charge transfer resistance of Bi NPs@Gr-CNTs was significantly reduced, which can be attributed to the remarkable electronic conducting properties of graphene and CNT. As a result, the Bi NPs@Gr-CNTs exhibited an enhanced electrocatalytic ability towards Hg (II). Bauskar and Rice [18] investigated the use of Bi/CNT/C electrodes in direct formic acid fuel cells (DFAFCs) and found that the combination of Bi with CNT resulted in the formation of functional groups that enhance electron conductivity. Furthermore, Bi decoration enhanced the electrocatalytic activity and the stability of DFAFCs. Zhang et al. [19] prepared Cu-doped BiO_x composites and used them in Fenton-like systems to degrade 2-chlorophenol. The system using Cu_2O as catalyst exhibited a removal rate of only 24%, whereas the system with the $BiCux/Bi^0$ catalyst designated as Bi/Cu molar ratio of 9 exhibited removal rate of 75%. Wang et al. [20] synthesized the bismuth-titanium alloy nanoparticles and composited them with porous carbon matrix (Bi-Ti@C) as a Cl-storage electrode, indicating that no serious structural changes have occurred in the electrode even after 100 cycles of electrochemical desalination (EDI). The introduction of Ti and carbon nanocages enhanced the binding force of the electrode, providing high stability during the repeated chlorination/dechlorination process. Wei et al. [21, 22] pointed out that the Bi-based complex oxides, such as $BiFeO_3$ and $Bi_2Fe_4O_9$ are suitable for application as heterogeneous catalysts in the photo-Fenton process. This is attributed to their excellent visible-light-driven property and the presence of iron element. Because of the synergistic effect between $BiFeO_3$ and $Bi_2Fe_4O_9$, the bentonite-based bismuth ferrites ($BiFeO_3$-$Bi_2Fe_4O_9$/Bent) displayed higher photocatalytic activity than $BiFeO_3$, which promoted e^- and h^+ to separate under visible light. In summary, the literature represents the advantages of Bi catalysts that could be utilized to expand their application scope in the EF process.

In previously study, we have preliminary demonstrated that the feasibility and benefits of using Bi modified CNT composite on Ti as electrode in advanced oxidation process [23]. Therefore, the main purpose of this study was to thoroughly analyze the characteristics of cathode via a series of qualitative and electrochemical analyses, exploring the effects of Bi electrodeposition time on the distribution of Bi deposits on the MWCNT. The electrochemical techniques were used to deposit multi-walled carbon nanotube (MWCNT) and Bi onto Ti substrates in order to construct composite Bi/MWCNT-coated Ti cathodes that possess three-dimensional structures. Our aim is to create an electrode that has outstanding electrochemical characteristics, which can enhance the performance of the Bi/MWCNT/Ti cathode in an EF system toward the degradation of the wastewater.

2. Materials and Methods

2.1. Preparation of the Cathode Substrate Surface. Ti substrates (length: 80 mm; width: 25 mm; thickness: 0.7 mm; purity ≥99.5%, Anatech Company Ltd., Taipei City, Taiwan) were polished using #100, #240, #400, #600, #800, and #1000-grit water sandpaper in this order. Ti substrates were then washed in an ultrasonic cleaner filled with acetone and distilled water to remove all oily substances and grime. The cleaned Ti substrates were then corroded using 75% H_2SO_4 for 30 min at 80°C.

2.2. Electrophoretic Deposition of MWCNT. In this experiment, the commercial multi-walled carbon nanotube (MWCNT, diameter: 10~20 nm, length: 5~15 μm, purity ≥95.0%, TCI Chemistry, Tokyo Chemical Industry Co., Ltd., Japan) was functionalized via acid modification to form well-dispersed MWCNT suspension. To this end, MWCNTs were added to a 3 : 1 mixture of sulfuric acid/nitric acid

(Nihon Shiyaku Industries Ltd., Japan), and its temperature was maintained at 70°C for 30 min. The acid-modified MWCNT was then used to prepare the MWCNT precursor solution by adding 50 mg of the functionalized MWCNT to 100 mL of ethanol. A magnetic stirrer was used to stir the solution until the MWCNT dissolved completely. Next, ultrasonication was conducted to ensure uniform MWCNT dispersion in the solution. The resulting solution is the precursor for electrophoretic deposition. A two-electrode system was used for the electrophoretic deposition of MWCNT, the Ti substrate was used as the anode, and Pt was used as the cathode. The electrophoretic deposition of MWCNT onto the Ti substrate was performed over 2 min at a DC voltage of 15 V (MWCNT/Ti).

2.3. Electrodeposition of Bi. The electrodeposition precursor consisted of bismuth nitrate (($Bi(NO_3)_3$, Nihon Shiyaku Industries Ltd., Japan), acetic acid (HAc, Nihon Shiyaku Industries Ltd., Japan), and sodium acetate (NaAc, Nihon Shiyaku Industries Ltd., Japan). HAc and NaAc were used for adjusting the pH of precursor to 4.5, while $Bi(NO_3)_3$ was used to provide the Bi^{3+} ions for the formation of the Bi deposits. The Bi-containing compound, HAc, NaAc, and the selected buffer solution were mixed in a specific ratio to form the Bi electrodeposition precursor solution, which requires 100 ppm of Bi^{3+}, some amount of HAc-NaAc solution, and 500 mL of deionized water.

The precursor solution was electrodeposited onto Ti with MWCNT using the ex situ method in a three-electrode system. The system consisted of a MWCNT-modified Ti cathode (working electrode), a Pt anode (auxiliary electrode), and an Ag/AgCl reference electrode. The electrodeposition precursor solution was prepared as previously described, and an external potential was then applied for varying periods of time to perform Bi electrodeposition (Bi/MWCNT/Ti).

2.4. Analysis of Material Characteristics. A Hitachi S-4800 (Tokyo, Japan) high-resolution scanning electron microscope (SEM) and a QUANTAX Annular XFlash® QUAD FQ5060 (Bruker, Middlesex, NJ, USA) energy-dispersive X-ray spectrometer (EDS) were used to investigate the effects of the deposition time on the surface morphology and atomic ratio of Bi; X-ray diffractometry (XRD) with Cu K_α radiation ($\lambda = 0.154$ nm) was performed using a Rigaku Ultima IV X-ray diffractometer, which was used to identify the chemical composition of electrode, with a scan rate of 2°/min and scan range of 20° to 80°.

2.5. Analysis of Electrochemical Characteristics. All the measurements for electrochemical characteristics were performed using an electrochemical workstation (Zive SP1 WonATech Co., Seoul, Korea). Cyclic voltammetry (CV) was performed to determine electron transfer rates for each electrode's reactivity with respect to Fe^{2+}/Fe^{3+} with the three-electrode system: CE (Pt, 20 mm × 40 mm, purity ≥99.9%, Anatech Company Ltd., Taipei City, Taiwan), RE (Ag/AgCl electrode, Anatech Company Ltd., Taipei City, Taiwan), and WE. The WE was either a Ti, MWCNT/Ti, or Bi/MWCNT/Ti electrode. Electrolyte was containing 1 M potassium chloride (KCl, Nihon Shiyaku Industries, Japan) and 0.01 M potassium ferricyanide ($K_3[Fe(CN)_6]$, Nihon Shiyaku Industries, Japan), and the pH of electrolyte was adjusted to 3.0. The scan range was +1 V~−1 V vs. Ag/AgCl. All the samples were performed under the same conditions and scan rates of 10, 25, 50, and 100 mV/s.

Linear sweep voltammetry (LSV) was performed to investigate the potential and current response of each electrode for oxygen reduction reaction (ORR). Three electrodes were used, as per CV. Electrolyte was 0.1 M KNO_3 with pH adjusted to 3.0. The solution was aerated for 10 min prior to the LSV tests to increase the dissolved O_2 (purity ≥99.0%) content. Scan range of 0 V to −1 V vs. Ag/AgCl and scan rate of 10 mV/s were used.

2.6. Analysis of Dye Decolorization Rates and Kinetics. A dual-chamber EF system was used with Pt counter electrode; Ag/AgCl reference electrode (Anatech Company Ltd., Taipei City, Taiwan); and working electrode. In each run, the WE was Ti, MWCNT/Ti, or Bi/MWCNT/Ti electrode, respectively. The chambers are linked by Pt wires passing through the glass walls, to complete the cell circuit. The CE chamber was filled with 0.1 M KNO_3 as electrolyte. The EF reaction takes place in the WE chamber. The WE chamber was filled with 0.1 M KNO_3 containing 20 mg/L $FeSO_4{\cdot}7H_2O$ (ACROS Organics, Belgium), and the pH value of electrolyte was adjusted to 3.0. Rhodamine B dye (Rh B, Sigma Aldrich Ltd., USA) was used as reagent to evaluate degradation efficiency, at 5 ppm initial concentration. Rh B concentration was measured using a UV-Vis spectrophotometer (Shishin SH-U880, Taiwan). During the experiment, the stirring rate was set to 600 rpm, supplying O_2 into electrolyte at 50 sccm by peristaltic pump simultaneously.

3. Results and Discussion

3.1. Electrodeposition of Bi on MWCNT-Coated Ti Cathodes. For depositing metallic ions onto a cathode at a constant electrodeposition potential, the selection of appropriate potential is important as it provides the driving force for ionic flow toward the cathode and subsequent ionic reduction and deposition onto the cathode. Cyclic voltammetry was conducted to analyze the redox reactions occurring between the electrodes and the electrolyte and to infer the state of electrodeposited Bi on the basis of the electrode's current responses. Figure 1 shows the potential-current graph that was recorded at the MWCNT/Ti electrode during cyclic voltammetry in the Bi electrodeposition electrolyte, and the potential sweep range was +1.0 V~−1.0 V vs. Ag/AgCl. The sweep initially proceeded toward negative potential before returning to the crossover point and then toward positive potentials. During the negative potential sweep, reductive current started to respond significantly at −0.45 V vs. Ag/AgCl, this corresponds to the reduction of Bi^{3+} on the cathode surface, and a current peak is observed

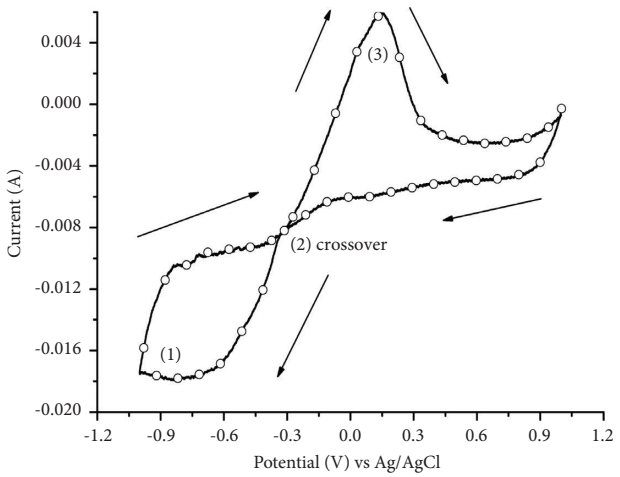

Figure 1: Cyclic voltammetry graph of the electrodeposition of Bi.

when the potential achieved −0.85 V vs. Ag/AgCl (1), exhibiting that the maximum reductive current without H_2 evolution promotes the reduction of Bi^{3+} [24]. The potential sweep switched directions at −1.0 V vs. Ag/AgCl, and a crossover occurred at (2) during the positive potential sweep, which shows that nucleation reactions still occurred on the electrode surface despite the presence of an oxidative current. Hence, Bi^{3+} reduction occurred on the electrode surface even when an oxidative current was present. As the oxidative potential increased, the nucleation reaction eventually ceased and resulted in a significant oxidative peak at (3). This indicates that oxidation occurred in the previously accumulated deposits, which then dissociated from the electrode surface, thus generating a large oxidative current. As the oxidation of reactants on the electrode surface is not limited by mass transfer, the oxidative current increased sharply with increasing potential [25].

Based on cyclic voltammetry results for the redox reactions at the MWCNT/Ti cathode in the electrodeposition precursor, it is shown that the maximum reduction peak occurs at −0.85 V vs. Ag/AgCl. The crossover point indicates that nucleation reactions occurred between the electrodeposition precursor and cathode, thus confirming that Bi can be deposited on the cathode surface by the precursor solution. According to Faraday's law of electrolysis, the magnitude of the current response is proportional to the rate of reactant deposition. Because the abovementioned analysis indicates that an electrodeposition potential of −0.85 V vs. Ag/AgCl gives the maximum current response for a MWCNT/Ti electrode in the Bi electrodeposition precursor, Bi electrodeposition onto MWCNT-coated Ti electrodes was performed at this potential.

3.2. Characterization of Bi/MWCNT/Ti Cathodes. In 3.1 Section, Bi/MWCNT/Ti cathode was designed through electrodeposition of Bi onto MWCNT/Ti electrode at an electrodeposition potential of −0.85 V vs. Ag/AgCl, and the effects of different deposition times on Bi/MWCNT/Ti cathodes was investigated further. The surface morphologies of Bi/MWCN/Ti cathodes prepared by 3, 5, and 7 min were observed at 10,000 magnifications by SEM, as shown in Figures 2(a)–2(c). In the SEM images of the cathode that underwent 3 min of Bi electrodeposition (denoted as Bi/MWCNT/Ti-3 min), it displayed the Bi microcrystals sparsely adhered on the surface of MWCN/Ti, and a partial aggregation tendency for Bi particles was also observed. After functionalizing MWCNT, the oxygen-containing functional groups with negative charge can provide more surface reaction sites to facilitate the cation adsorption, which provides the surface of nanotube for the function of incorporating additional substance [10]. In other words, it can promote the discrete adsorption of Bi^{3+} onto the surface of MWCNT and subsequently reduce it to Bi particles during electrodeposition, which further makes adhesion of Bi particles onto the MWCNT. On the electrode that underwent 5 min of Bi electrodeposition (Bi/MWCNT/Ti-5 min), the Bi particles had a particle-like appearance, the staggered and partially stacked flakes may be observed among the MWCNT, and the metallic Bi also formed long and slender needle-like structures on the MWCNT. Additionally, the formation of Bi deposits is significantly increased and more uniformly distributed than those on the Bi/MWCNT/Ti-3 min electrode. On the electrode that underwent 7 min of Bi electrodeposition (Bi/MWCNT/Ti-7 min), the number of particle-like metallic Bi significantly reduced, as these particles are replaced by dendrites. According to Su et al. [26], Bi is initially electrodeposited as aggregated particles, which will grow into dendrites if the electrodeposition time is extended. On the MWCNT surface, Bi grew in a continuous manner and began to form dendritic structures as electrodeposition continued.

Energy-dispersive spectroscopy (EDS) was performed to confirm the presence of Bi on the composite electrode after Bi electrodeposition. It is found that the Bi/MWCNT/Ti-3 min cathode had a Bi component, but at a lower content than Ti. This indicates that a relatively small amount of Bi was electrodeposited in 3 min. The Bi/MWCNT/Ti-5 min cathode showed a wider area of Bi adhesion as well as particle-like Bi deposits among the MWCNT. However, the aggregated Bi particles on its surface were small. The Bi deposits formed upon 5 min of Bi electrodeposition were uniform and particle-like, with a small number of dendrites. The atomic percentage of Bi on this electrode is 37.7%, respectively, which indicates that Bi adhesion is significantly stronger on the Bi/MWCNT/Ti-5 min cathode than that on the Bi/MWCNT/Ti-3 min cathode. Unlike the other cathode, the Bi/MWCNT/Ti-7 min cathode showed clear dendritic growth that covers the entire MWCNT surface. The atomic percentage of Bi on its surface is 59.78%, respectively, implying that the Bi/MWCNT/Ti-7 min cathode has the highest Bi content among the three Bi/MWCNT/Ti cathodes.

The composition of each cathode was determined by X-ray diffraction (XRD) analysis. The XRD patterns of the substrate and modified cathodes are shown in Figure 3. The Ti XRD pattern (black solid line) shows peaks at 70.94°, 53.34°, and 40.48°, which correspond to the (103), (102), and (101) crystal planes sequentially [27]. The MWCNT/Ti XRD pattern (red solid line) also shows three peaks at 53.38°,

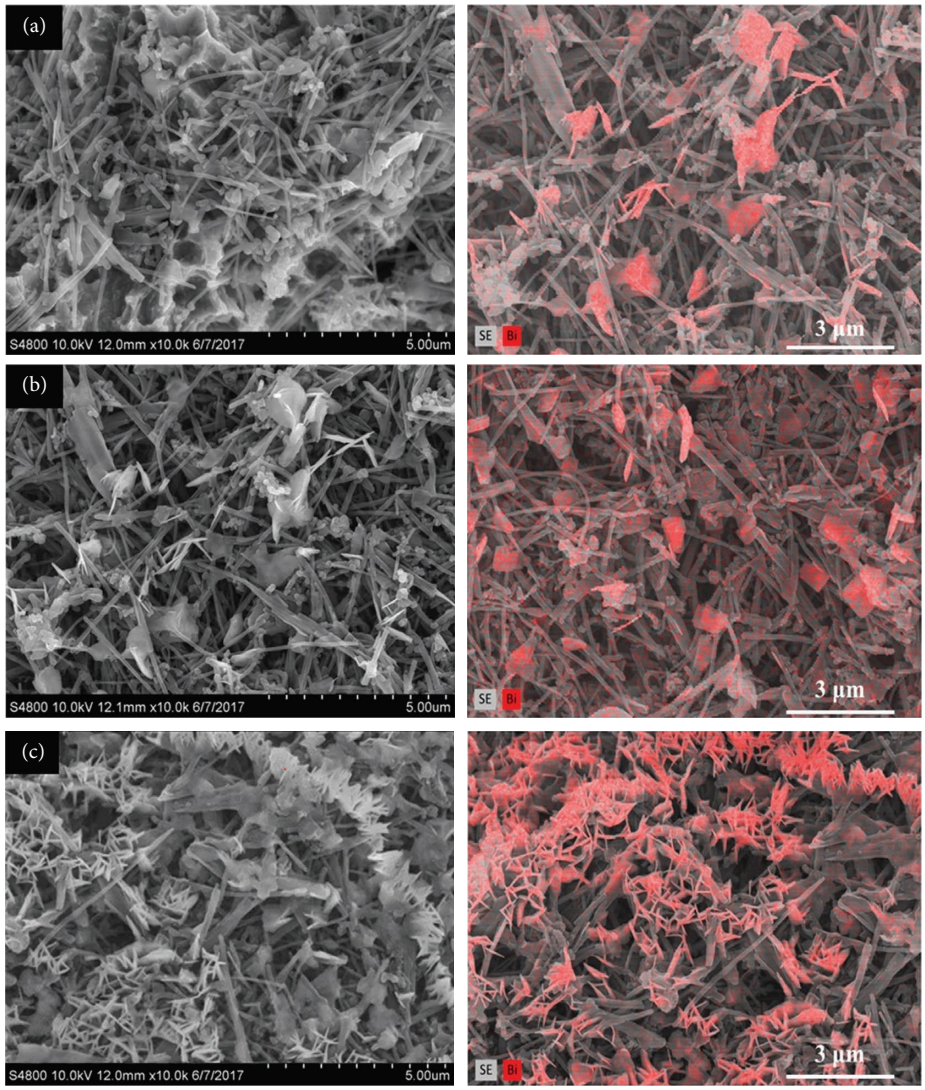

Figure 2: Surface morphologies of the Bi/MWCNT/Ti cathodes prepared at Bi electrodeposition times of (a) 3 min, (b) 5 min, and (c) 7 min.

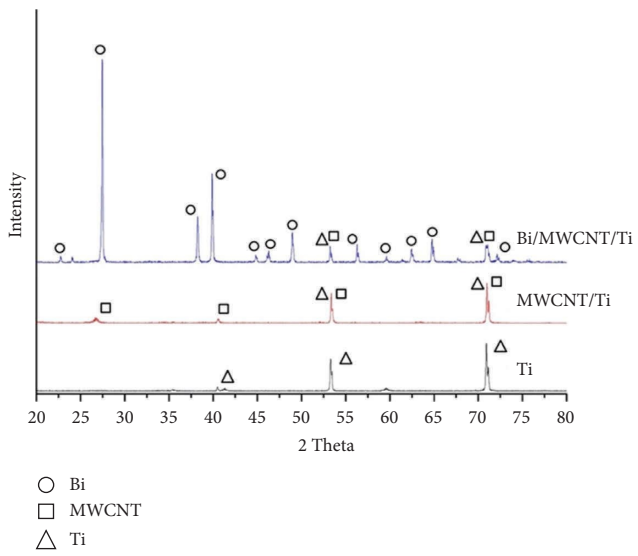

Figure 3: XRD patterns of the cathodes.

40.62°, and 26.66°, which correspond to the (004), (100), and (002) crystal planes, respectively. The Bi/MWCNT/Ti XRD pattern (blue solid line) displayed variety of peaks, which correspond to different crystal planes, and it is represented in Table 1 [20]. It may be observed that the peak at 27.64° is the most intense of these peaks. These results confirm that both MWCNT and Bi adhered on the Bi/MWCNT/Ti cathode. Therefore, a potential of −0.85 V vs. Ag/AgCl was found to be suitable for the electrodeposition of Bi onto the surface of MWCNT/Ti cathodes. It is also proven that the electrophoretic deposition of MWCNT onto the surface of the Ti substrate is successful; the presence of crystal plane peaks that correspond to metallic Bi in the XRD pattern of the Bi/MWCNT/Ti cathode further confirms that metallic Bi was deposited onto the surface of the MWCNT.

Figures 4(a)–4(e) illustrate the contact angle for variety of cathode. It is shown that the contact angle of the Ti substrate is 98.6°, which indicates that the surface of Ti is hydrophobic. The measured contact angle for the MWCNT/Ti cathode is 40.1°, indicating that MWCNT modification

Table 1: The crystal plane corresponding to the diffraction peak for Bi/MWCNT/Ti cathode.

2 theta	62.46°	56.30°	48.98°	46.30°	44.82°	39.90°	38.22°	27.64°	22.74°
Crystal planes	(107)	(024)	(202)	(006)	(105)	(110)	(104)	(012)	(003)

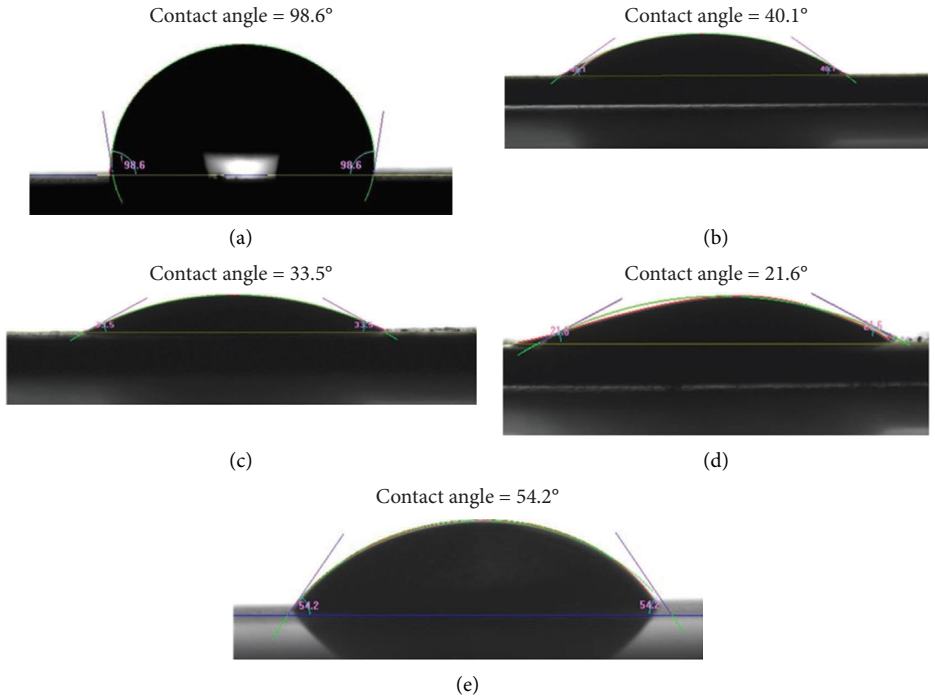

Figure 4: Contact angle measurements of (a) Ti, (b) MWCNT/Ti, (c) Bi/MWCNT/Ti-3 min, (d) Bi/MWCNT/Ti-5 min, and (e) Bi/MWCNT/Ti-7 min electrodes.

reduced the contact angle of the Ti cathode, which can attribute to the functionalization for MWCNT before electrophoretic deposition. The functionalization process introduces oxygen-containing functional groups to the surface of MWCNT, creating surface reaction sites and transforming the MWCNT into a hydrophilic surface. This improvement addresses the drawback of the chemical inertness and hydrophobicity of pristine MWCNT [10, 28]. The contact angles of the Bi/MWCNT/Ti-3 min, Bi/MWCNT/Ti-5 min, and Bi/MWCNT/Ti-7 min cathodes are 33.5°, 21.6°, and 54.2°, respectively, which indicate that these cathodes are even more hydrophilic than the MWCNT/Ti cathode. Ouyang et al. [15] constructed a Bi-film-wrappedsingle-walled CNT-modified glassy carbon electrode (Bi/SWNTs/GCE) for heavy metal detection in water and demonstrated that the modification of GCEs with Bi particles reduces their contact angle from 84.1° to 63.7°. The deposition of SWNTs (to form the Bi/SWNTs/GCE composite electrode) further reduced the contact angle to 11.5°, and it attributed to the carboxylic-group-functionalized SWNTs and metallic Bi imparted excellent compatibility with aqueous solutions. The SEM images of the Bi/MWCNT/Ti-3 min and Bi/MWCNT/Ti-5 min cathodes show that their Bi deposits are all particle-like, which explains why these cathodes have lower contact angles and higher hydrophilicity than the those of MWCNT/Ti cathode. However, extending the Bi electrodeposition time to 7 min resulted in a higher contact angle than that of the Bi/MWCNT/Ti-5 min cathode, which may be caused by the formation of Bi dendrites. It was noted by Su et al. that the hierarchical structure and low surface free energy of Bi dendrites induce hydrophobicity [26]. Hence, we conclude that the dendritic structures of the Bi/MWCNT/Ti-7 min cathode are responsible for its hydrophobicity.

3.3. Electrochemical Performance of the Bi/MWCNT/Ti Cathode. To evaluate the electrochemical performance of cathode in EF system, the electron transfer rates for varying deposition times of the Bi/MWCNT/Ti cathodes were measured by cyclic voltammetry, at scan rates of 10, 25, 50, and 100 mV/s (see Figures 5(a)–5(c)). In these figures, it is shown that the current responses for the oxidation and reduction peaks become stronger with increasing scan rate in all three Bi/MWCNT/Ti cathodes. Therefore, the Bi/MWCNT/Ti cathodes were capable of catalyzing reversible Fe(II)/Fe(III) redox reactions. Regression analyses were performed between peak current and the square root of scan rate (see equations (4) and (5), where I_p is the current density (A cm^{-2}), n is the stoichiometric number of electrons involved in the electrochemical reaction, A is the cathode area (cm^2), C is the concentration of the reactant in the solution, D is the diffusion coefficient of the reactant, v is the scan rate (V s^{-1}), and k' is the electron transfer rate).

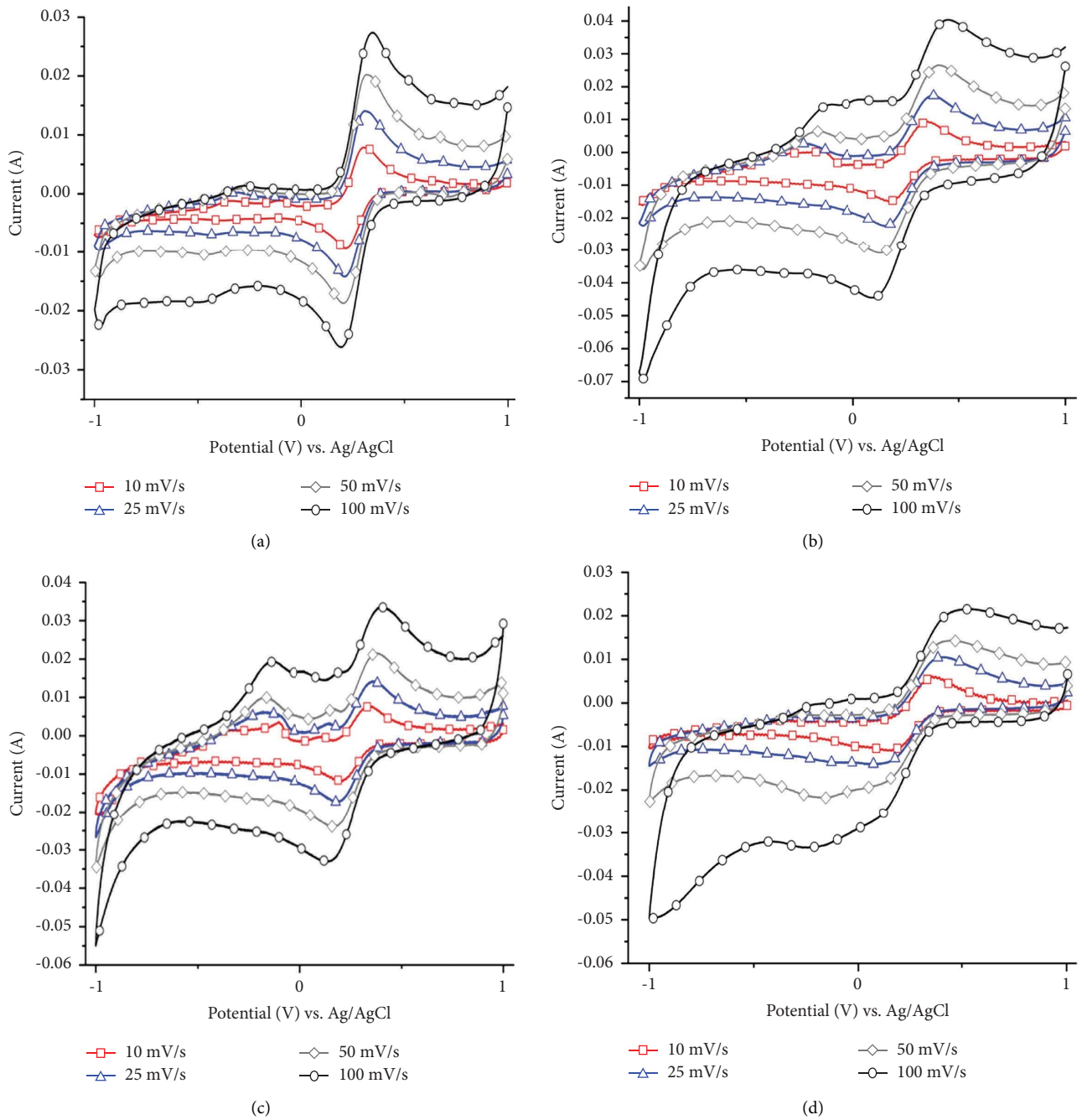

Figure 5: Continued.

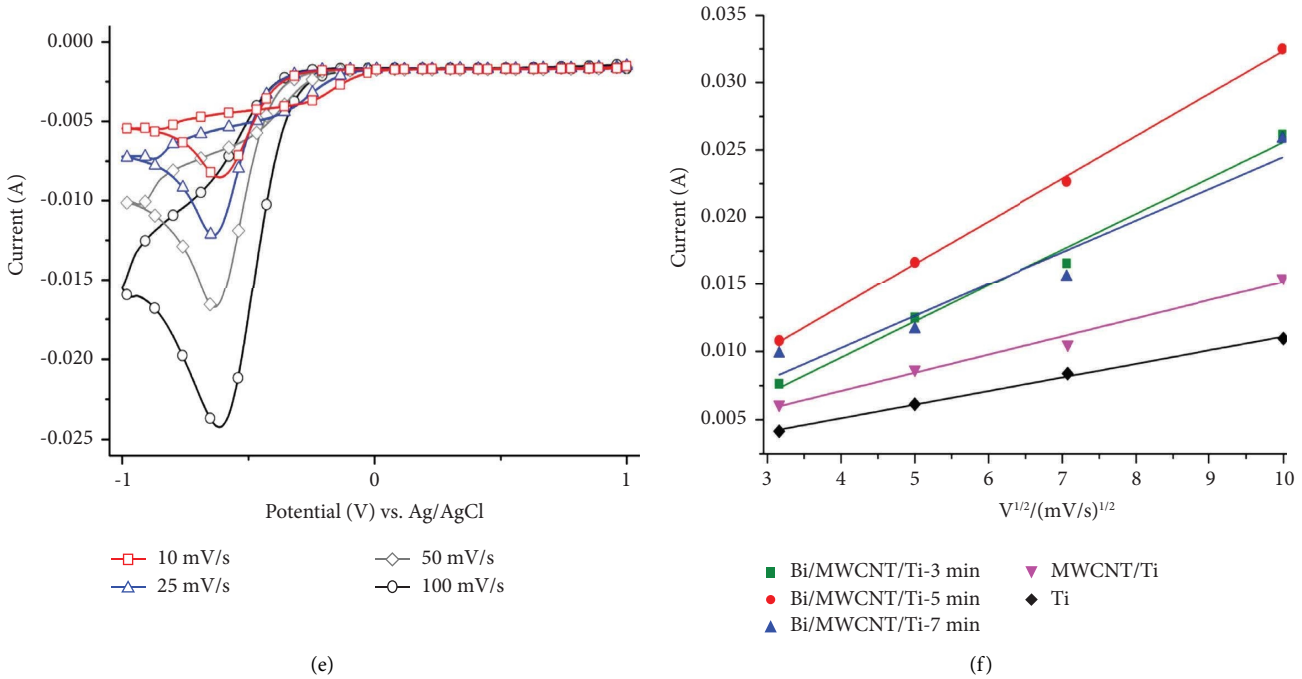

Figure 5: Electrocatalytic activity of cathode toward Fe(III)/Fe(II) redox reactions. (a) Bi/MWCNT/Ti-3 min. (b) Bi/MWCNT/Ti-5 min. (c) Bi/MWCNT/Ti-7 min. (d) MWCNT/Ti. (e) Ti. (f) Relationship between peak current and the square root of scan rate for each cathode.

The result revealed linear correlations with the coefficients of determination (R^2) of 0.98, 0.99, and 0.93 for the Bi/MWCNT/Ti-3 min, Bi/MWCNT/Ti-5 min, and Bi/MWCNT/Ti-7 min cathodes, respectively. On the other hand, the residuals between the predicted and measured values are only 10^{-4}, 10^{-5}, and 10^{-3}. Furthermore, the current responses of the peaked are enhanced for all of cathodes, indicating that the electrode performs a good reversible electrochemical reaction in the system. It can be observed that the response current of Bi/MWCNT/Ti cathodes is proportional to the square root of the scan rate, which is indicative of a typical diffusion-controlled electrochemical process [29]. Therefore, the peak current is given by equation (5). k' is the electron transfer rate of the cathode; the higher the value of k', the higher the electron transfer rate of the cathode in the system. The k' values of the Bi/MWCNT/Ti-3 min, Bi/MWCNT/Ti-5 min, and Bi/MWCNT/Ti-7 min cathodes are 26.6, 31.6, and 23.6, respectively. Figures 5(d) and 5(e) show the redox reactions for the MWCNT/Ti cathode and unmodified Ti cathode at various scan rates. The peak currents for these cathodes were linearly fitted to the square root of the scan rates, which resulted in the R^2 values of 0.98 and 0.99 for the MWCNT/Ti and Ti cathodes, respectively, and residuals of approximately 10^{-4}. Therefore, the current density of these cathodes is proportional to the square root of scan rate, and the k' values of the MWCNT/Ti and Ti cathodes are 13.4 and 10.0, respectively. Chang et al. [29] prepared CNT and Bi co-doped PbO_2 electrodes (CNT-Bi-PbO_2) and probed their electrochemical characteristics and stability; they found that the CNT-Bi-PbO_2 electrode showed significant oxidative and reductive current responses in cyclic voltammetry experiments. Hence, the CNT-Bi-PbO_2 electrode has excellent electrocatalytic activity toward Fe(III)/Fe(II) redox reactions. It is found that using Bi composited to MWCNT to modify the Ti cathode, the k' value can be significantly increased from 10.0 to 31.6.

$$I_p = 2.69 \times n^{3/2} \times A \times C \times D^{1/2} \times v^{1/2}, \quad (4)$$

$$I_p = k' \times v^{1/2}. \quad (5)$$

The linear sweep voltammetry curves of the Bi/MWCNT/Ti cathodes are shown in Figure 6. At −1.0 V vs. Ag/AgCl, the current responses of the Bi/MWCNT/Ti-3 min, Bi/MWCNT/Ti-5 min, and Bi/MWCNT/Ti-7 min cathodes are 30, 36, and 25 mA, respectively. At −1.3 V vs. Ag/AgCl, side reactions such as the HER began to occur at the Bi/MWCNT/Ti-3 min and Bi/MWCNT/Ti-7 min cathodes [30]. The side reactions began to occur at the Bi/MWCNT/Ti-5 min cathode when the potential achieves −1.5 V vs. Ag/AgCl; as the HER inhibits H_2O_2 generation [31], the presence of these side reactions has deleterious effects on the efficiency of the EF system. According to Le et al. [32], on highly hydrophilic electrode surfaces, aqueous O_2 moves toward the electrode and is adsorbed onto its surfaces, thus forming O_2(ads). This facilitates the movement of dissolved O_2 in the aqueous solution toward the cathode surface. Furthermore, the electrons received by the cathode will drive the ORR and, thus, generate H_2O_2. Figure 7 shows the linear sweep voltammetry curves of the Ti, MWCNT/Ti, and Bi/MWCNT/Ti (Bi/MWCNT/Ti-5 min) cathodes. It is shown that the Ti cathode begins to produce a reductive current at −0.5 V, and its H_2O_2 current response at the working potential of the EF process was

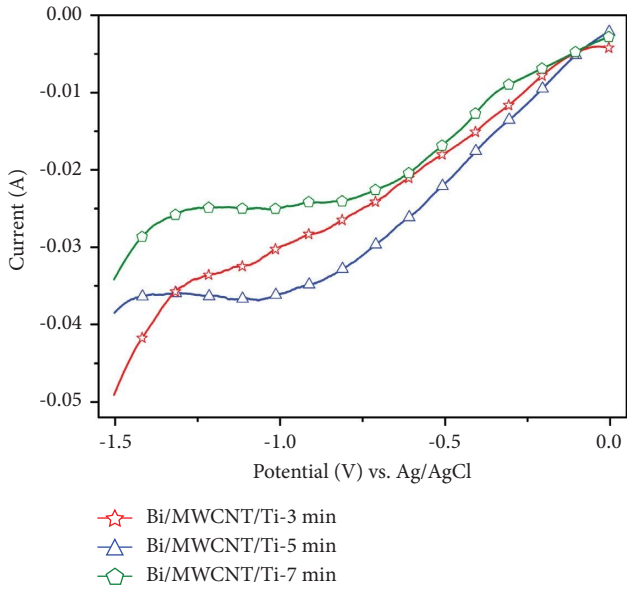

Figure 6: Linear sweep voltammetry curve of Bi/MWCNT/Ti-3 min, Bi/MWCNT/Ti-5 min, and Bi/MWCNT/Ti-7 min cathodes.

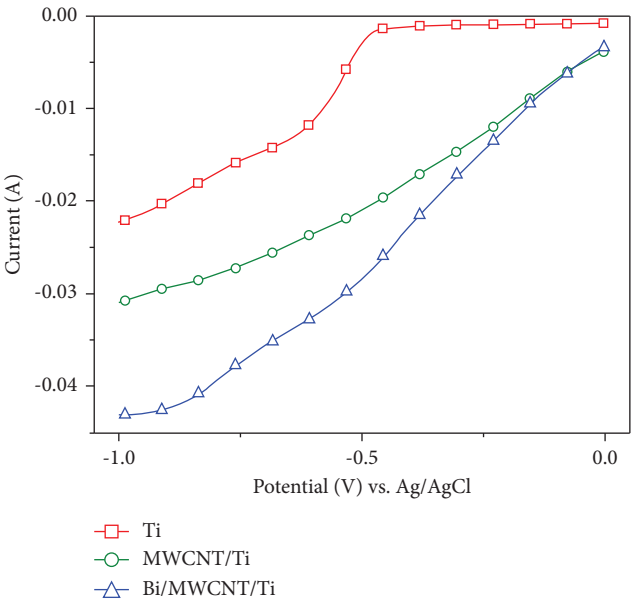

Figure 7: Linear sweep voltammetry curves of Ti, MWCNT/Ti, and Bi/MWCNT/Ti cathodes.

~20 mA. The MWCNT/Ti and Bi/MWCNT/Ti cathodes generated reductive currents at lower potentials, and their current responses at the working potential were 23 and 30 mA, respectively. Mousset et al. [33] noted that in linear sweep voltammetry experiments, net current is driven by the ORR that involves the transfer of two electrons to O_2 to form H_2O_2. Therefore, the aqueous solution contains dissolved O_2, and the larger the response current, the higher the ORR activity. Given that the Bi/MWCNT/Ti cathode has a higher current response than the Ti and MWCNT/Ti cathodes, it follows Faraday's law of electrolysis and the ORR activity of the cathodes.

3.4. Performance of Bi/MWCNT/Ti Cathode in EF. To determine the electrocatalytic activities of the Ti, MWCNT/Ti, and Bi/MWCNT/Ti cathodes toward the EF process, they were used as cathodes in EF systems. Rh B was added to the area around the cathodes, and changes in Rh B absorbance were recorded. The reaction rate of each cathode was derived from the Rh B degradation rate. Among the Bi/MWCNT/Ti cathodes prepared with three deposition time of Bi, the Bi/MWCNT/Ti-5 min cathode was selected for this experiment because it possesses high surface and electrochemical characteristics. A spectrophotometer was used to measure the changes in Rh B absorbance, and the degradation efficiency of each EF system was calculated using equations (6) and (7).

$$\eta = \frac{[\text{Rh B}]_t - [\text{Rh B}]_O}{[\text{Rh B}]_O}, \tag{6}$$

$$\ln \frac{[\text{Rh B}]t}{[\text{Rh B}]_O} = -\text{kt}. \tag{7}$$

In these equations, η is the degradation rate (%), $[\text{Rh B}]_0$ is the initial absorbance of Rh B, $[\text{Rh B}]_t$ is the absorbance value at time t, and k is the reaction rate. The degradation rates of each EF cathode are shown in Figure 8. Here, it is shown that the degradation rate of Rh B by the EF process after 30 min was 44.0% with the Ti cathode, 69.7% with the MWCNT/Ti cathode, and 80.8% with the Bi/MWCNT/Ti cathode.

In Figure 9, the natural log of [Rh B] to $[\text{Rh B}]_0$ was plotted against t to analyze the Rh B degradation kinetics of each cathode. The experiments performed in this work were analyzed according to equation (7). The result showed that all the R^2 values of linear regressions achieved 0.99, which implies that Rh B degradation reaction for Ti, MWCNT/Ti, and Bi/MWCNT/Ti has conformed to first-order reaction kinetics in the EF system. Liu et al. [34] doped PbO_2 electrodes with Bi to prepare Ti/Bi-PbO_2 composite electrodes for the electrocatalytic oxidation of o-nitrophenol (o-NP), m-nitrophenol (m-NP), and p-nitrophenol (p-NP); they found that 120 min of operation was required to fully remove the pollutants. The linear regressions that describe the oxidation of o-NP, m-NP, and p-NP with the Ti/Bi-PbO_2 electrode have R^2 values of 0.97, 0.97, and 0.9, respectively, which are consistent with first-order reaction kinetics. Furthermore, the residuals of the linear regressions for Ti, MWCNT/Ti, and Bi/MWCNT/Ti are only 10^{-4}, 10^{-3}, and 10^{-3}, respectively. As the slope for the linear regression corresponds to the reaction rate, it was found that the reaction rates of the Rh B degradation reaction with the Ti, MWCNT/Ti, and Bi/MWCNT/Ti cathodes were 0.0195, 0.04219, and 0.05579, respectively. Hence, Rh B degradation was most rapid in the EF system using the Bi/CNT/Ti cathode; this trend is consistent with the measurement of cyclic voltammetry and linear sweep voltammetry.

In summary, the use of metallic Bi in EF cathodes improves the efficiency of the EF process. The electrodeposition of Bi onto the MWCNT/Ti cathode further improved the degradation rate to 80.8%. All three cathodes exhibited the

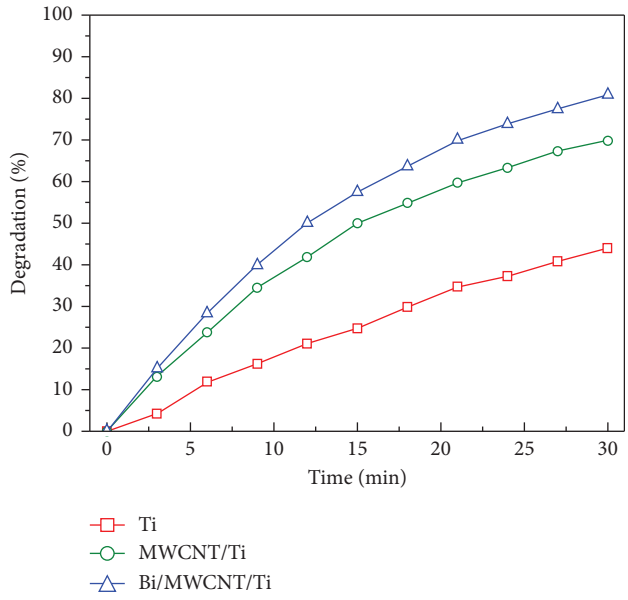

Figure 8: Degradation of Rh B dye by EF systems with Ti, MWCNT/Ti, and Bi/MWCNT/Ti cathodes.

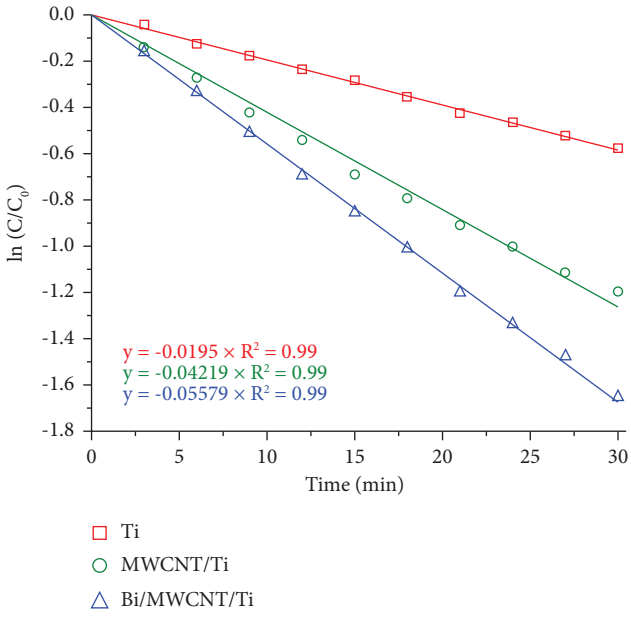

Figure 9: Kinetics of Rh B degradation by EF systems with Ti, MWCNT/Ti, and Bi/MWCNT/Ti cathodes.

first-order reaction kinetics, and the EF system with the Bi/MWCNT/Ti cathode exhibited the highest Rh B degradation rate.

4. Conclusions

In this study, we revealed a composite technique to prepare the cathode with excellent hydrophilicity and catalytic performance of cathode. Among then, it was found that Bi particles exhibited staggered and partially stacked flakes for Bi/MWCNT/Ti cathode prepared for 5 minutes of electrodeposition, which could be observed on the surface of MWCNT, and it possesses the lowest contact angle (21.6°). Further, a long electrodeposition time leads to form dendrites structure of Bi that grew continuously on the surface of the MWCNT, causing the cathode trends to lower hydrophilicity. The electron transfer rate of the Bi/MWCNT/Ti-5 min cathode is measured as 31.6 by cyclic voltammetry. The linear sweep voltammetry measurements indicated that Bi/MWCNT/Ti-5 min showed the highest response current. Using the Bi/MWCNT/Ti cathode, an Rh B degradation rate of 80.8% was achieved, which is approximately 1.81 times higher than Ti cathode; it exhibited that the metallic Bi effectively improved the kinetic rate for Ti cathode in EF system. We report the technique with low temperature and controllable composite electrode preparation, which can be developed potentially for cathode in advanced oxidation processes.

Data Availability

The data used to support the findings of this study are available from the corresponding author upon reasonable request.

Conflicts of Interest

The authors declare that they have no conflicts of interest.

Acknowledgments

The authors sincerely appreciate the financial support from National Science and Technology Council, R.O.C. (NSTC), under grant nos. MOST-110-2221-E-197-029 and MOST-111-2221-E-197-014-MY2.

References

[1] M. Corona-Bautista, A. Picos-Benítez, D. Villaseñor-Basulto, E. Bandala, and J. M. Peralta-Hernández, "Discoloration of azo dye Brown HT using different advanced oxidation processes," *Chemosphere*, vol. 267, Article ID 129234, 2021.

[2] J. Casado, "Towards industrial implementation of Electro-Fenton and derived technologies for wastewater treatment: a review," *Journal of Environmental Chemical Engineering*, vol. 7, no. 1, Article ID 102823, 2019.

[3] W. Liu, Z. Ai, and L. Zhang, "Design of a neutral three-dimensional electro-Fenton system with foam nickel as particle electrodes for wastewater treatment," *Journal of Hazardous Materials*, vol. 243, pp. 257–264, 2012.

[4] E. Brillas, I. Sirés, and M. A. Oturan, "Electro-Fenton process and related electrochemical technologies based on Fenton's reaction chemistry," *Chemistry Review*, vol. 109, no. 12, pp. 6570–6631, 2009.

[5] I. Sirés and E. Brillas, "Upgrading and expanding the electro-Fenton and related processes," *Current Opinion in Electrochemistry*, vol. 27, Article ID 100686, 2021.

[6] J. Lee, A. Son, Y. J. Ko et al., "Investigation of titanium mesh as a cathode for the electro-Fenton process: consideration of its practical application in wastewater treatment," *Environ Sci Water Res Technol*, vol. 6, pp. 1627–1637, 2020.

[7] Q. Lu, G. S. Hutchings, W. Yu et al., "Highly porous non-precious bimetallic electrocatalysts for efficient hydrogen

evolution," *Nature Communications*, vol. 6, pp. 6567-6568, 2015.

[8] W. Sun, N. Yu, J. Chen, Z. Gu, J. Wei, and Y. Yao, "Heterogeneous Ti/PbO2-electro-Fenton degradation of aromatic methane dyes using industrial pyrite waste slag as catalyst," *Environmental Science & Pollution Research*, vol. 29, no. 33, pp. 50218–50236, 2022.

[9] S. Yuan, N. Gou, A. N. Alshawabkeh, and A. Z. Gu, "Efficient degradation of contaminants of emerging concerns by a new electro-Fenton process with Ti/MMO cathode," *Chemosphere*, vol. 93, no. 11, pp. 2796–2804, 2013.

[10] B. Sarkar, S. Mandal, Y. F. Tsang, P. Kumar, K. H. Kim, and Y. S. Ok, "Designer carbon nanotubes for contaminant removal in water and wastewater: a critical review," *Science of the Total Environment*, vol. 612, pp. 561–581, 2018.

[11] H. Roth, Y. Gendel, P. Buzatu, O. David, and M. Wessling, "Tubular carbon nanotube-based gas diffusion electrode removes persistent organic pollutants by a cyclic adsorption–electro-Fenton process," *Journal of Hazardous Materials*, vol. 307, pp. 1–6, 2016.

[12] A. Khataee, M. Safarpour, M. Zarei, and S. Aber, "Electrochemical generation of H2O2 using immobilized carbon nanotubes on graphite electrode fed with air: investigation of operational parameters," *Journal of Electroanalytical Chemistry*, vol. 659, no. 1, pp. 63–68, 2011.

[13] H. Shi, C. Tang, Z. Wang et al., "Nanoporous bismuth electrocatalyst with high performance for glucose oxidation application," *International Journal of Hydrogen Energy*, vol. 46, no. 5, pp. 4055–4064, 2021.

[14] Y. Tian, L. Hu, S. Han, Y. Yuan, J. Wang, and G. Xu, "Electrodes with extremely high hydrogen overvoltages as substrate electrodes for stripping analysis based on bismuth-coated electrodes," *Analytica Chimica Acta*, vol. 738, pp. 41–44, 2012.

[15] R. Ouyang, W. Zhang, S. Zhou et al., "Improved Bi film wrapped single walled carbon nanotubes for ultrasensitive electrochemical detection of trace Cr (VI)," *Electrochimica Acta*, vol. 113, pp. 686–693, 2013.

[16] Y. Miao, Z. Yang, X. Liu et al., "Self-assembly of BiIII ultrathin layer on Pt surface for non-enzymatic glucose sensing," *Electrochimica Acta*, vol. 111, pp. 621–626, 2013.

[17] N. Jeromiyas, E. Elaiyappillai, A. S. Kumar, S. T. Huang, and V. Mani, "Bismuth nanoparticles decorated graphenated carbon nanotubes modified screen-printed electrode for mercury detection," *Journal of the Taiwan Institute of Chemical Engineers*, vol. 95, pp. 466–474, 2019.

[18] A. S. Bauskar and C. A. Rice, "Spontaneously Bi decorated carbon supported Pd nanoparticles for formic acid electrooxidation," *Electrochimica Acta*, vol. 107, pp. 562–568, 2013.

[19] L. Zhang, L. Lyu, Y. Nie, and C. Hu, "Cu-doped Bi2O3/Bi0 composite as an efficient Fenton-like catalyst for degradation of 2-chlorophenol," *Separation and Purification Technology*, vol. 157, pp. 203–208, 2016.

[20] H. Wang, H. Gang, D. Wei et al., "Bismuth–titanium alloy nanoparticle@porous carbon composite as efficient and stable Cl-storage electrode for electrochemical desalination," *Separation and Purification Technology*, vol. 296, Article ID 121375, 2022.

[21] G. Wei, Y. Yang, Y. Li et al., "A new catalytic composite of bentonite-based bismuth ferrites with good response to visible light for photo-Fenton reaction: application performance and catalytic mechanism," *Applied Clay Science*, vol. 184, Article ID 105399, 2020.

[22] G. Wei, Y. Yang, Y. Li, L. Zhang, Z. Li, and R. Mo, "Improving the catalytic activity of bentonite-based bismuth ferrites composite via mechanical activation for photo-Fenton process," *Materials Chemistry and Physics*, vol. 260, Article ID 124118, 2021.

[23] Y. T. Wang, Y. C. Hsieh, and Y. S. Lin, "Performance of bismuth modified carbon nanotube composite titanium electrode in advanced oxidation process system," in *Proceedings of the 2019 IEEE International Conference on Consumer Electronics-Taiwan (ICCE-TW)*, pp. 1-2, IEEE, Yilan, Taiwan, June 2019.

[24] E. Sandnes, M. E. Williams, U. Bertocci, M. Vaudin, and G. Stafford, "Electrodeposition of bismuth from nitric acid electrolyte," *Electrochimica Acta*, vol. 52, no. 21, pp. 6221–6228, 2007.

[25] M. S. Martín-González, A. L. Prieto, R. Gronsky, T. Sands, and A. M. Stacy, "Insights into the Electrodeposition of Bi[sub 2] Te[sub 3]," *Journal of the Electrochemical Society*, vol. 149, no. 11, p. C546, 2002.

[26] C. Su, Z. Lu, H. Zhao, H. Yang, and R. Chen, "Photoinduced switchable wettability of bismuth coating with hierarchical dendritic structure between superhydrophobicity and superhydrophilicity," *Applied Surface Science*, vol. 353, pp. 735–743, 2015.

[27] D. Gu, Y. C. Hagedorn, W. Meiners et al., "Densification behavior, microstructure evolution, and wear performance of selective laser melting processed commercially pure titanium," *Acta Materialia*, vol. 60, no. 9, pp. 3849–3860, 2012.

[28] J. Macko, N. Podrojková, R. Oriňaková, and A. Oriňak, "New insights into hydrophobicity at nanostructured surfaces: experiments and computational models," *Nanomaterials and Nanotechnology*, vol. 12, Article ID 184798042110623, 2022.

[29] L. Chang, Y. Zhou, X. Duan, W. Liu, and D. Xu, "Preparation and characterization of carbon nanotube and Bi co-doped PbO2 electrode," *Journal of the Taiwan Institute of Chemical Engineers*, vol. 45, no. 4, pp. 1338–1346, 2014.

[30] P. Liang, M. Rivallin, S. Cerneaux, S. Lacour, E. Petit, and M. Cretin, "Coupling cathodic Electro-Fenton reaction to membrane filtration for AO7 dye degradation: a successful feasibility study," *Journal of Membrane Science*, vol. 510, pp. 182–190, 2016.

[31] Y. Wang, Y. Liu, K. Wang, S. Song, P. Tsiakaras, and H. Liu, "Preparation and characterization of a novel KOH activated graphite felt cathode for the electro-Fenton process," *Applied Catalysis B: Environmental*, vol. 165, pp. 360–368, 2015.

[32] T. X. H. Le, M. Bechelany, S. Lacour, N. Oturan, M. A. Oturan, and M. Cretin, "High removal efficiency of dye pollutants by electron-Fenton process using a graphene based cathode," *Carbon*, vol. 94, pp. 1003–1011, 2015.

[33] E. Mousset, Z. Wang, J. Hammaker, and O. Lefebvre, "Physico-chemical properties of pristine graphene and its performance as electrode material for electro-Fenton treatment of wastewater," *Electrochimica Acta*, vol. 214, pp. 217–230, 2016.

[34] Y. Liu, H. Liu, and Y. Li, "Comparative study of the electrocatalytic oxidation and mechanism of nitrophenols at Bi-doped lead dioxide anodes," *Applied Catalysis B: Environmental*, vol. 84, no. 1-2, pp. 297–302, 2008.